Spatial Filters on Demand Based on Aperiodic Photonic Crystals

Darius Gailevičius, Vytautas Purlys, Martynas Peckus, Roaldas Gadonas, and Kestutis Staliunas*

Photonic Crystal spatial filters, apart from stand-alone spatial filtering function, can also suppress multi-transverse-mode operation in laser resonators. Here it is shown that such photonic crystals can be designed by solving the inverse problem: for a given spatial filtering profile. Optimized Photonic Crystal filters were fabricated in photosensitive glass. Experiments have shown that such filters provide a more pronounced filtering effect for total and partial transmissivity conditions.

1. Introduction

Spatial filtering by Photonic Crystals (PhC), due to extremely small dimensions of such filters, is a very promising technique for micro-optical applications. Such filters allow improvement of the spatial quality of the light beams without significantly increasing the size and complexity of the system. Typical dimensions of conventional spatial filters (a confocal arrangement of two lenses with an iris in confocal plane) extend at least several centimeters, meanwhile the length of the PhC based spatial filters can be made of the order of 100 μm. The physical mechanism of PhC filtering is also different: the conventional spatial filters require a direct access to spatial Fourier spectrum of propagating beam (at a confocal plane), while the PhC filtering does not require direct operations in the far field. This makes the PhC spatial filters potentially applicable for improving the spatial characteristics of powerful lasers, where the conventional filtering is problematic due to thermal problems of tightly focused beam. This also makes the PhC filters especially attractive for intracavity spatial filtering in micro-lasers and micro-resonators, where a conventional filter simply can not be placed.

The originally proposed PhC spatial filtering[1] relies on the angular bandgaps in a Bragg diffraction configuration. Such filtering has been demonstrated in optics,[1,2] and in acoustics by so called sonic crystals[3]). For visible and near infrared optics the Bragg configuration is inconvenient from the fabrication viewpoint, as it requires the longitudinal periods $2d_z$ of the structure to be smaller than the wavelength λ ($d_z < \lambda$, see **Figure 1**). This is a severe limitation for various fabrication techniques, including the direct writing by femtosecond pulses. Alternatively, the spatial filtering can be realized in the Laue diffraction configuration, as proposed in,[4] where the longitudinal periods exceed the wavelength ($d_z > \lambda$). Spatial filtering in Laue configuration was demonstrated in different PhC geometries,[5,6] see also the recent review.[7] Such filters have been also shown to provide transverse mode selection in a microchip laser by introducing losses for higher order transverse modes and improving beam quality by several times.[8]

The Laue configuration does not lead to the conventional angular bandgaps, as the diffracted wave components propagates to the same direction as the incident beam. The diffracted wave components, therefore, in course of propagation, couple back into the incident beam, resulting to Rabi-like oscillations between the near-axis- and diffracted wave components. This results not in complete angular bandgaps, but in quasi-bandgaps. The filtering angles can be calculated following the wave Talbot-resonance conditions: specifically that the angular component with $\mathbf{k} = (k_x, k_z)$ and $k^2 = k_x^2 + k_z^2 = \omega^2/c^2$, subjected to the diffraction on wavevector $\mathbf{q} = (q_x, q_y)$, results in a scattered wave $\mathbf{k}_1 = \mathbf{k} + \mathbf{q}$ which is also resonant: $k_1^2 = \omega^2/c^2$. In paraxial approximation this results in a simple expression:

$$\sin(\alpha) = (Q-1)\cdot q_x/(2k_0) = (Q-1)\cdot \lambda/(2d_x)\,, \tag{1}$$

where the dimensionless coefficient $Q = 2d_x^2/(\lambda d_z)$ is a PhC geometry parameter.

The Rabi-oscillatory character of Laue diffraction imposes the limitation on the length of the PhC: the optimum length is approximately: $L = 2\cdot\lambda/\Delta n_{\mathrm{ref}}$, and the angular width of the line is limited to $\Delta\phi = \sqrt{3}\cdot\Delta n_{\mathrm{ref}}\cdot d_x/(2\lambda)$, where Δn_{ref} is refraction index contrast. Also the filtering line is of a bell-profile for $z < L$, but an oscillatory or even disordered for $z > L$. For many applications one needs broader/narrower angular ranges of filtering, also frequently the filtering line should have a particular shape, for instance a rectangle.

One of the possible solutions to broaden the angular quasi-bandgap is to use the chirped PhCs. As the filtering angle

D. Gailevičius, V. Purlys, M. Peckus, and R. Gadonas
Laser Research Center, Department of Quantum Electronics
Vilnius University
Sauletekio Ave. 10, LT-10222, Vilnius, Lithuania
E-mail: Darius.Gailevicius@ff.vu.lt

K. Staliunas
DONLL, Departament de Física
Universitat Politècnica de Catalunya (UPC)
Edifici Gaia, Rambla Sant Nebridi 22, 08222 Terrassa, Spain

Institució Catalana de Recerca i Estudis Avançats (ICREA)
Passeig Lluís Companys 23, 08010 Barcelona, Spain

DOI: 10.1002/andp.201700165

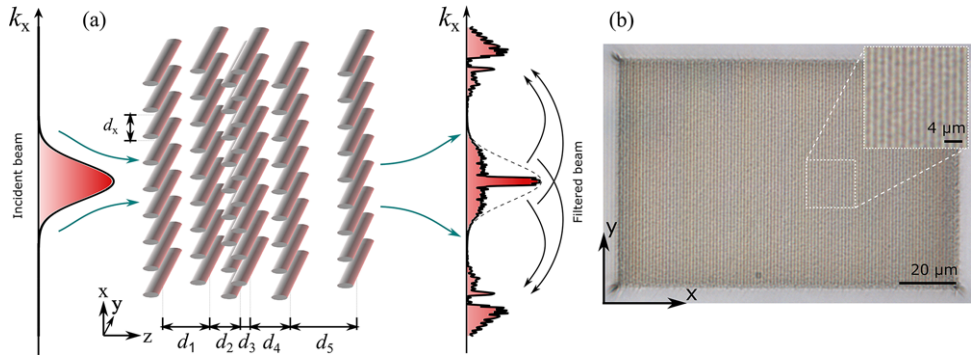

Figure 1. The PhC spatial filtering concept. (a) shows the side-view of the incident beam propagation through the aperiodic optimized PhC, where the planes of modified refractive index plane structures are placed at different positions $d_1, d_2 \ldots d_n$. (b) the optical microscopy image of the PhC embedded in glass (top-view).

depends on the periods of the structure it is in principle possible to design a structure where the period smoothly varies along the PhC, and respectively the filtering line adiabatically sweeps through the required angular range. This allows to increase the angular range of spatial filtering.[6] however the shape of the filtering line is hardly controllable.

Here we propose a principally different scenario of engineering the angular quasi-bandgaps in PhCs: instead of attempting to systematically calculate the chirped structure, we use the optimization algorithm to design the PhC according to the required spatial filtering characteristics. In a simplest case such characteristics can be the width and depth of the dips in the angular transmission curve, while in a more sophisticated case one can define an exact shape of the angular transmission function. Different applications have different requirements for the spatial filtering line: for instance the intracavity PhC filters in high finesse resonators[8] do not require 100% filtering (zero transmission), but rather shallow and broad dips in the transmission function.

We use an optimization algorithm to engineer the angular transmission function of the PhCs on demand. The rest of the letter is devoted to the calculation, fabrication, and measurement of such PhC filter with required characteristics. In concluding part we also show the potential of the algorithm to design more sophisticated shapes of spatial filtering.

2. Methods

2.1. Numeric optimization

The PhCs have been designed using a numerical optimization based on steepest descent algorithm. The interlayer distances (in longitudinal direction) of the structure were subjected to variation. In order to maintain the transverse translational invariance, we kept a transverse period constant and equal to $d_x = 1.2\,\mu$m. We defined an interlayer distance vector $\mathbf{d} = (d_1, d_2, d_3, \ldots, d_{(n-1)}, d_n)$, as a set of longitudinal (in the propagation direction) layer spacings. A fitness function $F(\mathbf{d})$ has been introduced that defines how well the spatial transmittance spectrum $T(\alpha, \mathbf{d})$ corresponds to a target ("ideal") spatial transmission spectrum. The target transmission spectrum in most cases was defined to be equal to 1 in a central angular band $|\alpha| < |\alpha_1|$, and was restricted to exceed a predefined value T_{max} in an angular range (band) $\alpha_1 \leqslant |\alpha| \leqslant \alpha_2$ (in Supporting Information we show more sophisticated transmission functions). We thus define the fitness function as:

$$F^{-1}(\mathbf{d}) \triangleq \int_{-\delta_2}^{+\delta_2} \left(T(\delta, \mathbf{d}) - T_t(\delta)\right)^2 \cdot G(\delta) \cdot H\left[T(\delta, \mathbf{d}) - T_{\max}\right] \, \mathrm{d}\delta \,. \quad (2)$$

In order to deal with a dimensionless fitness function, we use a normalized wave-vector projection value $\delta = k_x/k_0 = k_x\lambda/2\pi = \arcsin\alpha$. In addition, to ensure that the more relevant angular components will lead to a larger impact we use a weight function that corresponds to the probe beam angular intensity profile (we considered it Gaussian as most generic: $G(\delta) = \exp(-\delta^2/\delta_0^2)$,).

We also restrict the range of d_i values to minimum and maximum ones $d_{\min}$, $d_{\max}$. The lower bound, specifically $d_{\min} = 2.4\,\mu$m, is empirically determined by the limits of fabrication (the resolution). The upper bound $d_{\max} = 10.9\,\mu$m, is set somewhat arbitrarily limiting the maximum possible dimensions of the PhC. We solve the optimization problem using an interior-point solver as described in,[9–11] gradients were approximated using forward differences and second derivatives either with forward differences or where possible with the Broyden-Fletcher-Goldfarb-Shanno algorithm. The optimization starts from a predefined initial vector $\mathbf{d_0}$ and at each iteration the angular transmission profile for a given $\mathbf{d}$ is computed by a modified beam propagation method approach (see eq. (S9) in Supporting information) and compared to the target transmittance function $T_t(\delta)$ and the $\mathbf{d} = \mathbf{d} + \Delta$ value is updated to a presumably more optimal value.

We consider two relevant cases: 100% low angle pass filtering $T_{\max} = 0\%$. The other case is $T_{\max} = 50\%$, where we keep in mind that for many applications, e.g. laser resonators not necessarily 100% filtering is needed. For this reason in eq. (2) the integral argument features a step (Heaviside H) function. We note that not only the bounds can be selected in multiple ways, but also the the optimization method itself.

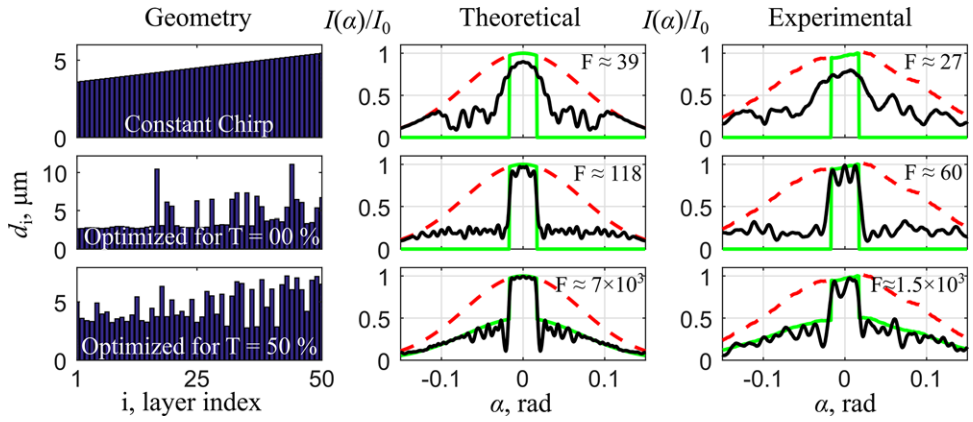

Figure 2. Numerical and experimental results compared. We show the cases for constant chirp and optimized for both $T_{max} = 50\%$ and 0%. Numerically derived angular intensity spectra and experimentally derived spectra are shown.

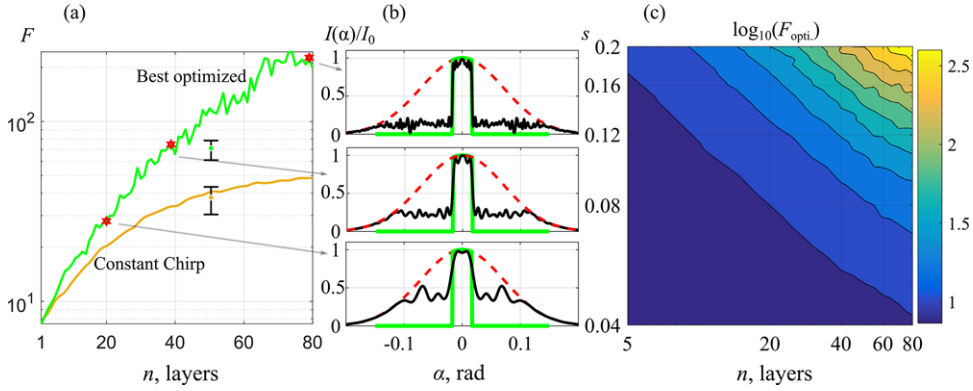

Figure 3. (a) Optimized geometry fitness values vs. the initial chirped and periodic PhC cases, where we show (b) numeric intensity profiles expected for selected cases. Together we show (c) fitness values dependence on the s parameter and number of layers n (computations were limited to maximum 400 iterations per point).

2.2. Fabrication and Measurements

Fabrication of PhCs was performed by a point-by-point modification of refractive index using a tightly focused femtosecond laser beam using a DLW setup, described more in detail in.[6] The DLW method is widely used for inscription of various micro-optical and photonic components in glass, such as waveguides,[12] Bragg gratings,[13] also a variety of other structures and materials.[14] The PhCs were fabricated in Foturan glass $n_{ref} = 1.52$ (a lithium-aluminum-silicate based photoetchable glass). This material is frequently used for etching of micro-fluidic channels or tailoring light transmission by controlling the volume of laser/light exposed volume.[15,16] For our experiments we did not apply the annealing step, as it decreases the filtering function of the fabricated PhCs, due to diffusion of laser affected regions and scattering by nanocrystallites. However, we took the advantage of the higher refractive index change resulting in untreated Foturan glass compared to the soda-lime or borosilicate glass, and lower scattering compared to the fused silica, where the scattering is very pronounced due to formation of nanogratings.[17]

For fabrication we used 300 fs duration pulses from Yb:KGW laser providing 1030 nm wavelength radiation and focused it with a 1.25 NA microscope objective. Pulse repetition rate was 10 kHz and beam translation speed was 250 μm/s. The optimal laser power was 1 mW (after the objective) with a pulse energy of $E_p = 100$, nJ and an approximate peak intensity at the focus $I_{peak} \approx 42\,TW/cm^2$. We note that the scattering coefficient by one layer of the PhCs fabricated in such a way is $s \approx 0.13$ (see Supporting information for details).

For characterization of the filtering performance we probed the samples by linearly polarized continuous 633 nm wavelength He-Ne laser beam focused into the structure using a 0.25 NA objective. Angular divergence was 180 mrad (≈ 10 degrees). To explore the spatial filtering we recorded the beam far field profiles by CCD camera positioned at ≈ 10 mm distance behind the PhC.

3. Results

The experimental measurement results are summarized in **Figure 2** and **Figure 3**. Figure 2 shows the transmission characteristics of the designed structure, compared with the transmission by a chirped structure. The fitness F as defined for the $T_{max} = 0\%$ case is the worst for constant chirp, where the chirping interval is tuned to the filtering range from 17 mrad to 150 mrad and we

observe qualitative agreement and an improvement of performance for optimized cases. The imperfections of fabrication of the PhC structure result in lower F values compared to the numerically calculated cases. Also, the minimum interlayer distances are at the limit of the fabrication resolution, which is another source of the discrepancy. Nevertheless, we experimentally observed that for the 100% case ($T_{max} = 0\%$) the merit value increased by factor of $F_{Opt.,T=0}/F_{Chirp.,T=0} \approx 2$ times compared to the chirped case (see Fig. 3(a)). Furthermore, for the $T_{max} = 50\%$ filtering case the increase of performance from the chirped to optimized case is even larger $F_{Opt.,T=0.5}/F_{Chirp.,T=0.5} \approx 3$. To quantify the discrepancies we added random error to the optimal geometries, similarly as in [18] (see Note 4 in Supporting Information). By taking only the error for layer displacements into account, the amount of displacement needed to produce drastic changes for observable F would be of two magnitudes larger than for band-gap based structures.

Due to the fabrication restrictions the number of periods in fabricated structure was limited to $n = 50$ layers, which however can be increased by using more advanced fabrication techniques. Therefore we performed the numerical optimization of angular PhC filtering with the parameters beyond those fabrication restrictions in Foturan glass (which come out to be a more suitable glass compared to soda-lime glass used in our previous works.[6,8]) For Foturan, according to our estimations the single-layer scattering coefficient is: $s \approx 0.13$. In addition, we made calculations for longer crystals compared to those that we could presently fabricate. Figure 3 gives a quantitative summary of filtering efficiency dependence on the PhC length. The optimized values are calculated starting from the chirped case where the interlayer distances are distributed between the values of 3.585 to 5.71 μm. As the PhC length increases a steeper central pass boundary is achieved. In addition, different optimized solutions are always present for different initial chirp configurations. We note that these solutions are non-trivial such as in figure 2 and often feature non-smooth distribution of interlayer distances. We also show that if we were able to further increase the scattering efficiency parameter s and number of layers n, we could achieve even higher fitness values values (figure 3(c)).

4. Conclusions

Finally we remark the advantages of the method of spatial filtering by optimized PhC filters over the conventional filtering by confocal arrangement of lenses: i) the filters are of extremely small thickness (hundreds of microns), therefore they can fit into micro-optical devices or into resonators of micro lasers. ii) It is possible to combine the filtering functionality with other functionalities (such as amplification, or nonlinearities) in bulk material, by additional modulation of the refractive index of the (amplifying or nonlinear) material. iii) PhC spatial filter has no physical aperture limitations and no significant absorption that makes it very attractive for high power laser systems. iv) Translation invariance in lateral direction (insensitivity to the lateral shift of structure). v) Designs with different spatial transmittance profiles (soft or hard, narrow or wide) can be achieved by starting from basic constant-chirp variations.

Supporting Information

Supporting Information is available from the Wiley Online Library or from the author.

Acknowledgements

We acknowledge financial support by Spanish Ministerio de Educación y Ciencia and European FEDER (project FIS2015-65998-C2-01), NATO SPS 985048 research grant, European Union Horizon 2020 Framework EUROSTARS via project E10524 HIP-Laser.

Conflict of Interest

The authors delcare no conflict of interest.

Keywords

Beam shaping, spatial filtering, photonic crystal, numeric optimization, direct laser writing, glass, photostructurable glass

Received: May 3, 2017
Revised: May 22, 2017
Published online: July 3, 2017

[1] E. Colak, A. O. Cakmak, A. E. Serebryannikov, and E. Ozbay, *J. Appl. Phys.* **108**(11), 113106 (2010).
[2] Z. Tang, D. Fan, S. Wen, Y. Ye, and C. Zhao, *Chin. Opt. Lett.* **5**(S1), S211–S213 (2007).
[3] R. Picó, I. Pérez-Arjona, V. Sánchez-Morcillo, and K. Staliunas, *Appl. Acoust.* **74**(7), 945–948 (2013).
[4] K. Staliunas and V. J. Sánchez-Morcillo, *Phys. Rev. A* **79**(5), 053807 (2009).
[5] L. Maigyte, T. Gertus, M. Peckus, J. Trull, C. Cojocaru, V. Sirutkaitis, and K. Staliunas, *Phys. Rev. A* **82**(4), 043819 (2010).
[6] V. Purlys, L. Maigyte, D. Gailevičius, M. Peckus, M. Malinauskas, and K. Staliunas, *Phys. Rev. A* **87**(3), 033805 (2013).
[7] L. Maigyte and K. Staliunas, *Appl. Phys. Rev.* **2**(1), 011102 (2015).
[8] D. Gailevicius, V. Koliadenko, V. Purlys, M. Peckus, V. Taranenko, and K. Staliunas, *Sci. Rep.* **6**, 34173 (2016).
[9] R. H. Byrd, M. E. Hribar, and J. Nocedal, *SIAM J. Optim.* **9**(4), 877–900 (1999).
[10] R. H. Byrd, J. C. Gilbert, and J. Nocedal, *Math. Program.* **89**(1), 149–185 (2000).
[11] R. Waltz, J. Morales, J. Nocedal, and D. Orban, *Math. Program.* **107**(3), 391–408 (2005).
[12] G. D. Marshall, M. Ams, and M. J. Withford, Proc. SPIE, Vol. 6183 (2006), p. 61830Q.
[13] D. Grobnic, S. J. Mihailov, C. W. Smelser, and H. Ding, *IEEE Photonics Technol. Lett.* **16**(11), 2505–2507 (2004).
[14] M. Malinauskas, A. Žukauskas, S. Hasegawa, Y. Hayasaki, V. Mizeikis, R. Buividas, and S. Juodkazis, *Light: Science & Applications* **5**, e16133 (2016).
[15] S. Juodkazis, K. Yamasaki, V. Mizeikis, S. Matsuo, and H. Misawa, *Applied Physics A* **79**(4-6), 1549–1553 (2004).
[16] Z. L. Li, D. K. Y. Low, M. K. Ho, G. C. Lim, and K. J. Moh, *J. Laser Appl.* **18**(4), 320–324 (2006).
[17] Y. Shimotsuma, P. G. Kazansky, J. Qiu, and K. Hirao, *Phys. Rev. Lett.* **91**(24), 247405 (2003).
[18] D. M. Song, Z. X. Tang, L. Zhao, Z. Sui, S. C. Wen, and D. Y. Fan, *Chin. Phys. Lett.* **30**(4), 044206 (2013).

